Articles in PresS. Am J Physiol Gastrointest Liver Physiol (January 29, 2015). doi:10.1152/ajpgi.00114.2014

TITLE: Hydroxy-α sanshool induces colonic motor activity in rat proximal colon: a possible involvement of KCNK9 (104 Ch: limit 120)

SHORT TITLE: Hydroxy-α sanshool induces colonic motility (43Ch: limit 45)

Kunitsugu Kubota,[1)*] Nobuhiro Ohtake,[1)*] Katsuya Ohbuchi,[1,2)] Akihito Mase,[1)] Sachiko Imamura,[1)] Yuka Sudo,[2)] Kanako Miyano,[2)] Masahiro Yamamoto,[1)] Toru Kono,[3,4)] Yasuhito Uezono.[2)]

*These two authors equally contribute to this research.

1) Tsumura Research Laboratories, Tsumura & Co., Ibaraki, Japan.

2) Division of Cancer Pathophysiology, National Cancer Center Research Institute, Tokyo, Japan.

3) Department of Gastroenterology, Hokkaido University Graduate School of Medicine, Sapporo, Japan.

4) Center for Clinical and Biomedical Research, Sapporo Higashi Tokushukai Hospital, Sapporo, Japan.

CORRESPONDENCE TO: Yasuhito Uezono, M.D., Ph.D.

Division of Cancer Pathophysiology, National Cancer Center Research Institute

Tsukiji 5-1-1, Chuo-ku, Tokyo 104-0045, Japan

Tel: +81-3-3547-5248 Fax: +81-3-3542-1886

Email: yuezono@ncc.go.jp

KEYWORDS: hydroxy-α sanshool, two-pore domain potassium channels, KCNK9, KCNK3, colonic motility, long distance contraction, rhythmic propulsive motor complex, rhythmic propagating ripple, postoperative ileus

ABBREVIATIONS: AUC, area under the curve; CHO-K1, Chinese hamster ovary - K1; CM, circular muscle; DAPI, 4',6-diamidino-2-phenylindole; GI, gastrointestinal; HAS, hydroxy-α-sanshool; HBS, hydroxy-β-sanshool; ICC, interstitial cells of Cajal; ISH, *in situ* hybridization; LDC, long distance contraction; LID, lidocaine; LM, longitudinal muscle; MP, myenteric plexus; PF, peak frequency; POI, postoperative ileus; PPA, peak pressure amplitude; RPMC, rhythmic propulsive motor complex; RPR, rhythmic propagating ripple; SMC, smooth muscle cells; TRP, transient receptor potential; TRPA1, transient receptor potential ankyrin 1; TRPV1, transient receptor potential vanilloid type 1; TTX, tetrodotoxin; TU-100, daikenchuto.

GRANT SUPPORT AND DISCLOSURE: This project has been executed using the institutions' (National Cancer Center Research Institute and Tsumura & Co.) budgets including a grant from Tsumura & Co. providing to TK, YS, KM and YU for this collaborative research. KK, NO, KO, AM, SI and MY are the employees of Tsumura & Co.

AUTHOR CONTRIBUTIONS: KK and NO initiated and directed the entire study, designed experiments and wrote the manuscript; KO performed analysis of mRNA, two-electrode voltage clamp assay and membrane potential assay; AM performed *in vivo* experiments; SI contributed to immunohistochemistry experiments; MY performed immunohistochemistry experiments; YS, KM, MY and TK contributed to the experimental design; YU co-directed the entire study, analyzed data and wrote the manuscript.

ABSTRACT (250 words: limit 250)

Background and Aim: Various colonic motor activities are thought to mediate propulsion and mixing/absorption of colonic content. The Japanese traditional medicine daikenchuto (TU-100), which is widely used for postoperative ileus in Japan, accelerates colonic emptying in healthy humans. Hydroxy-α-sanshool (HAS), a readily absorbable active ingredient of TU-100 and a KCNK3/KCNK9/KCNK18 blocker as well as TRPV1/TRPA1 agonist, has been investigated for its effects on colonic motility. **Methods:** Motility was evaluated by intraluminal pressure and video imaging using rat proximal colons in an organ bath. Distribution of KCNKs was investigated by RT-PCR, *in situ* hybridization and immunohistochemistry. Current and membrane potential was evaluated using recombinant KCNK3- or KCNK9-expressing *Xenopus* oocytes and CHO cells. Defecation frequency in rats was measured. **Results:** HAS dose-dependently induced strong propulsive "squeezing" motility, presumably as long distance contraction (LDC). TRPV1/TRPA1 agonists induced different motility patterns. The effect of HAS was unaltered by TRPV1/TRPA1 antagonists and desensitization. Lidocaine (LID, a nonselective KCNKs blocker) and hydroxy-β-sanshool (HBS, a geometrical isomer of HAS and KCNK3 blocker) also induced colonic motility as a rhythmic propagating ripple (RPR) and a "LDC"-like motion, respectively. HAS-induced "LDC", but not LID-induced "RPR", was abrogated by a neuroleptic agent tetrodotoxin. KCNK3 and KCNK9 were located mainly in longitudinal smooth muscle cells and in

neural cells in the myenteric plexus (MP), respectively. Administration of HAS or TU-100 increased defecation frequency in normal and laparotomy rats. **Conclusions:** HAS may evoke strong LDC possibly *via* blockage of the neural KCNK9 channel in the colonic myenteric plexus.

INTRODUCTION

Control of the mechanical activity of the intestines is complex and our understanding of the mechanisms involved is still in its infancy. Elements of the regulation of motor activity and the electrical and mechanical properties of the intestines have been found to be different depending on the species, regions of intestines under investigation, conditions of the specimen (*in vivo* or *in vitro*, unstimulated or stimulated, etc.) and methodology used for evaluation. In the rat colon, several distinct motor patterns have been demonstrated by Huizinga and colleagues (3, 11). Among them, the patterns termed "rhythmic propulsive motor complex (RPMC)/long distance contraction (LDC)" and "rhythmic propagating ripple (RPR)" have been proposed to be created, at least partly, by two independent networks of interstitial cells of Cajal (ICC). It has been suggested that RPMC/LDC and RPR may be related to the propulsion and mixing/absorption of the luminal contents, respectively. Therefore, agents affecting these motor patterns could lead to the development of new therapeutic options for colonic dismotility diseases such as constipation.

TU-100, a pharmaceutical-grade traditional Japanese (kampo) medicine, has been widely used for the treatment of various gastrointestinal disorders including postoperative ileus and ischemic intestinal disorders (17). The drug has been approved as a prescription drug by the Ministry of Health, Labor and Welfare of Japan and integrated into the modern medical care system in Japan. A double-blind, placebo-controlled study on healthy volunteers in the U.S. has shown that treatment

89 with TU-100 significantly accelerates ascending colon emptying (22). Several double blind
90 placebo-controlled trials on the patients with postoperative ileus (POI), Crohn's disease, functional
91 constipation and irritable bowel syndromes are currently underway in the U.S. and Japan. The drug
92 is an extract powder made from a mixture of Japanese pepper, processed ginger and ginseng radix,
93 with maltose powder as an additive. Hydroxy-α-sanshool (HAS) contained in Japanese pepper has
94 been elucidated as one of the main active compounds responsible for the efficacy of TU-100 to POI
95 and adhesive intestinal obstruction (31, 32). Furthermore, HAS is rapidly absorbed in the gut and
96 reaches high concentrations in the blood when TU-100 is administered orally (12, 24, 25).
97 Hydroxy-β-sanshool (HBS), a geometrical isomer of HAS is also rapidly absorbed into the
98 bloodstream (12, 24, 25). HAS and HBS, which have been known as agonists to transient receptor
99 potential vanilloid type 1 (TRPV1) and transient receptor potential ankyrin 1 (TRPA1) (18), are now
100 recognized as selective blockers to certain two-pore domain potassium (KCNK) channels: HAS for
101 TASK-1 (KCNK3), TASK-3 (KCNK9) and TRESK (KCNK18) and HBS for KCNK3 (1).
102 TRPA1 expresses abundantly in enterochromaffin cells and TRPA1 stimulation induces serotonin
103 (5-HT) release resulting in enteric nerve activation (26), which may be a trigger for stimulus-induced
104 colonic motility (10). KCNK3 has been reported to express in colonic smooth muscle cells (SMC)
105 and to be involved in the determination of the resting potential (and therefore excitability) of SMC,
106 which may affect the contractility of colonic smooth muscle (28). In the present study, we

characterized the motility induced by HAS and investigated the mechanism of motility focusing on the possible involvement of TRP and/or KCNK channels.

MATERIALS AND METHODS

Chemicals and drugs

HAS, HBS, TU-100 and maltose were supplied by Tsumura and Co. Capsaicin (Sigma-Aldrich, St. Louis, MO), allyl isothiocyanate (AITC; Tokyo Chemical Industry, Tokyo, Japan), BCTC (COSMO BIO, Tokyo, Japan), HC-03003 (COSMO BIO), and lidocaine (LID; MP Biomedicals, Santa Ana, CA) were commercially obtained. Other chemicals were purchased from Wako Pure Chemical Industries, Osaka, Japan).

Animals

Male SD rats (Japan SLC, Hamamatsu, Japan) at 7-12 weeks old were housed under controlled light environmental conditions and had free access to food and water. All experimental procedures were ethically approved by the Laboratory Animal Committee of Tsumura and Co. and performed according to the institutional guidelines for the care and use of laboratory animals, which is in accordance with the National Institutes of Health Guide for the Care and Use of Laboratory Animals.

Isolated rat proximal colon tract and measurement of intraluminal pressure

Rats were fasted overnight and sacrificed by decapitation before removing their entire colon. A 2-cm to 3-cm segment of the proximal colon was placed into an organ bath (100 mL volume), which was continuously perfused with warm Krebs solution (3.5 mL/min, 34-5 °C). The oral and aboral ends of

the proximal colon segment were securely attached with string to an input and output port of the saline, respectively. In order to monitor intraluminal pressure (cmH_2O), a Mikro-Tip catheter pressure transducer (SPR-524, Millar Instruments, Houston, TX) was set in the lumen of the aboral end. Motility was initiated by loading an intraluminal pressure to approximately 4 cmH_2O by elevating the drain tube. After an equilibration period of 120-240 min, contraction had reached a consistent pattern, in terms of amplitude and frequency. The intraluminal pressure waves were evaluated by a data acquisition and analysis system (MP100, BIOPAC System, Goleta, CA). The motility was macroscopically observed through video images (PCR-SR87, SONY, Tokyo, Japan). All drug solutions were added to Krebs solution in the organ bath (serosal side). Peak frequency (PF) was calculated as the mean number of pressure peaks per minute during a defined period. The peak pressure amplitude (PPA) was calculated as the mean pressure of peaks during an allotted time period. The area under the curve (AUC) during the allotted time period was also calculated. The %-PF, % - PPA and %-AUC of each period were calculated as the ratio to the PF, PPA and AUC before drug treatment, respectively.

Spatiotemporal mapping

A “spatiotemporal map”, which is an image representation of motor activity, was generated according to the method described by Huisinga et al. (11). Colon width (coded as image intensity, black to white) is calculated at each point along the length of the colon (image Y-axis), for each

video frame (image X-axis) using ImageJ software. As shown in Figure 1C, propagating contractions are represented as the diagonal streaks of dark color. Broad relaxation is represented as white area.

RT-PCR

Muscle layer was carefully detached from the rat ascending colon and the remaining layer was used as the mucosal layer. Total RNA was prepared with RNeasy Universal Tissue Kit (QIAGEN, Hilden, Germany) and cDNA was synthesized with High Capacity cDNA Reverse Transcription Kits (Life Technologies) according to the manufacturer's instructions. Sequences of sense and anti-sense primers for RT-PCR analysis were as follows: rat KCNK3 sense: 5'-TCATCACCACAATCGGCTAT-3', anti-sense: 5'-AGCGCGTAGAACATGCAGAA-3', rat KCNK9 sense: 5'-CCTTCTACTTCGCTATCAC-3', anti-sense: 5'-CCAGCGTCAGAGGGATAC-3', KCNK18 sense: 5'-CTCACTTCTTCCTCTTCTTCTC-3', anti-sense: 5'-TAGCAAGGTAGCGAAACCTCT-3' and GAPDH sense: 5'-CGCATCTTCTTGTGCAGT-3', anti-sense: 5'-AATGAAGGGGTCGTTGATGG-3'. An aliquot of the RT reaction product served as a template in 30 cycles with 10 s of denaturation at 98°C, 30 s of annealing at 55°C, and 20 s of extension at 68°C using the DNA polymerase KOD FX (TOYOBO, Osaka, Japan). A portion of the PCR mixture was electrophoresed through a 2% agarose gel in Tris-acetate-EDTA buffer (pH 8.0), and the gel was stained with ethidium bromide and

imaged on a Typhoon 9410 imager (GE Healthcare, Piscataway, NJ).

***In situ* hybridization**

In situ hybridization (ISH) was performed by using QuantiGene ViewRNA. Gene specific probe sets for rat KCNK3, KCNK9, PGP9.5 mRNAs were designed by Affymetrix (Santa Clara, CA). Muscle layer was collected from rat ascending colon. Fixation and hybridization were conducted by GeneticLab (Sapporo, Japan). Hybridized target mRNAs were visualized using bright-field microscopy (BIOREV BZ-9000, Keyence, Osaka, Japan).

Immunohistochemistry

Whole mount immunohistochemistry was performed as follows: Intestinal specimens were opened along the mesenteric border. The specimens were stretched taut and pinned out flat to a silicone ring and fixed with ice cold acetone for 30 minutes. After fixation, each preparation was washed three times for 10 minutes each in phosphate-buffered saline (PBS; 0.9% NaCl in 0.1 M sodium phosphate buffer, pH 7.0). The preparations were placed in Superblock (Thermo Fischer Scientific, Rockford, IL) containing 0.3% Triton X-100 overnight at 4°C. The preparations were then placed in primary antibody diluted in antibody diluent (DAKO Japan, Tokyo, Japan) overnight at 4°C. After removal from the primary antibody, the tissues were rinsed for 3 × 10 minutes with PBS and incubated with the relevant secondary antibody conjugated to Alexa fluorochromes (Molecular Probes, Eugene, OR) diluted in antibody diluent (DAKO Japan) overnight at 4°C. After a final set of rinses, the

preparations were mounted on microslides and coverslipped with Prolong Gold antifade reagent (Molecular Probes). The slides prepared from whole mount or 7μm-thick sliced specimens were observed using confocal laser microscopy FV-100D (Olympus, Tokyo, Japan). The following antibodies were used: a mouse monoclonal antibody to KCNK9 (Sigma-Aldrich), a guinea pig polyclonal antibody to PGP9.5 (Abcam plc, Cambridge, UK), rabbit polyclonal antibodies to KCNK3 (Santa Cruz Biotechnology Inc. Dallas, TX), CD117 (DAKO Japan), platelet-derived growth factor receptor (PDGFR)-α (Santa Cruz Biotechnology) and smooth muscle actin and nuclei were visualized by staining with Alexa568-conjugated phalloidin and 4',6-diamidino-2-phenylindole (DAPI), respectively (Molecular Probes). In double immunostaining, each cell was identified by a combination of DAPI and a respective marker, and double positive- and single positive-cells were counted by visual inspection.

Preparation of plasmids and cRNAs

Rat KCNK3 cDNA was amplified from rat whole brain cDNA (Takara, Otsu, Japan) and introduced into pcDNA-DEST40 by Gateway system (Life Technologies, Carlsbad, CA). Rat KCNK9 cDNA was purchased from OriGene (Rockville, MD). cRNAs were prepared with mMessage mMachine Kit (Life Technologies) following the manufacturer's instructions.

Two-electrode voltage clamp assay

Immature V and VI oocytes from *Xenopus* were enzymatically dissociated. Isolated oocytes were

incubated at 18°C in ND-96 medium (96 mM NaCl, 2 mM KCl, 1.8 mM $CaCl_2$, 1 mM $MgCl_2$, 5 mM HEPES pH 7.4) containing 2.5 mM sodium pyruvate and 50 μg/mL gentamicin. Two-electrode voltage clamp assays were performed 2-4 days after cRNA injection. Currents were recorded with a GeneClamp 500 Amplifier (Molecular Probes, Sunnyvale, CA) and Digidata 1322A (Axon Instruments, New York, NY) and acquired using pCLAMP (Molecular Devices) software.

Membrane potential assay

Chinese hamster ovary (CHO)-K1 cells (ATCC, Manassas, VA) were seeded into 96well plates (~7,000cells/well). Rat KCNK3 or KCNK9 were then transiently expressed in CHO-K1 with FuGENE HD Transfection Reagent (Promega, Madison, WI) following the manufacturer's instructions. About 48hr after transfection, a membrane potential assay was performed using a FLIPR Membrane Potential Assay Kit (Molecular Devices). The change of membrane potential was monitored in terms of fluorescence intensity, measured using a FlexStation3 (Molecular Devices).

Analysis of defecation frequency

Normal Rats: HAS was orally administered and thereafter the rat's feces were counted cumulatively during a 5 hr period under fasting. **Laparotomy rats:** Rats (7 - 8 week old) were incised about 4 cm in the median line of the abdomen after being anesthetized by intraperitoneal injection of Somnopentyl (Kyoritsu Seiyaku, Tokyo, Japan). The small intestine, cecum and large intestine were exteriorized and covered with sterile gauze dampened with saline for 1 hr before

218 returning to the abdominal cavity and closing the abdomen. Rat feces were counted cumulatively
219 over a 7 hr period under the fasting state. Rats in the non-operation group were only anesthetized.
220 HAS and TU-100 were administered orally to rats by the gavage technique 3 or 4 hr after abdominal
221 closure.

222 **Data analysis**

223 All values are expressed as means ± SE. The statistical significance between 2 groups was evaluated
224 by F-test analysis of variance, followed by Student's t-test or Aspin-Welch's t-test. Statistical
225 significance between 3 or more groups was evaluated by Dunnett's test. When the agents were added
226 sequentially, repeated measure ANOVA was used. A probability of less than 0.05 was considered
227 statistically significant.

228

RESULTS

Evaluation of colonic motor activity by intraluminal pressure peaks and video imaging and effect of HAS

Motility of isolated segments of the proximal colon was analyzed by the measurement of intraluminal pressure and video image recordings. During a 2 hr period after the beginning of the experiment, moderate amplitude pressure peaks were observed (see Figure 1A). Thereafter the amplitude of these pressure peaks weakened and by the 3 hr time point only very small peaks could be detected (see Figure 1A, from time 3 hr to 4 hr). Nonetheless, low amplitude contractions were still detected by video imaging, which appeared to be propulsive (Figure 1A; details shown in the spatiotemporal map of Figure 1C) until the end of the experiment. These types of contractions do not always produce evident changes in pressure peaks. We performed quantitative analysis of colonic motility mainly by assessing changes in the pressure because they are in good agreement with the motility observed in video-imaging, at least for the high amplitude propagating motor activity. Relationship between the intraluminal pressure chart and the video images is shown in Supplementary Movie M1 and M2, and the relationship between the intraluminal pressure chart and spatiotemporal map is shown in Figure 1C. It should be noted that for the low amplitude motor activity, not all of the activity produces evident changes in the pressure peaks. Therefore, analyses based on the pressure peaks may tend to underestimate its frequency.

As shown in Figure 1A, addition of HAS to the bath solution from the serosal side at 30 min and 3 hr induced high amplitude periodic pressure peaks with similar frequency and potency. The motility is characterized by a strong squeezing over a broad range of the proximal colon (Figures 1B, 1C, movie files are shown in Supplementary Movie M3), after a brief temporal relaxation (Figure 1C). The dose-dependency of pressure peak pattern, PF, PPA and AUC are shown in Figure 2.

Contraction induced by HAS is not a result of stimulation of TRPV1/TRPA1

Firstly, we investigated whether TRPV1/TRPA1 agonists evoke motility similar to that induced by HAS. A TRPV1 agonist capsaicin (0.1 - 10 μM) evoked a single contraction peak only, both at 30 min (data not shown) and 3 hr (Figure 3A) though its PPA was potent. A TRPA1 agonist arylisothiocyanate (AITC) induced periodic contractions, although the amplitude was very small even at high concentrations (Figure 3B represents the result of AITC added at 100 μM at 3 hr; Supplementary Movie M5). Furthermore, administration of TRPV1 or TRPA1 inhibitor (BCTC and HC-030031, respectively), and desensitization of TRPV1/TRPA1 by bolus application of high doses of capsaicin plus AITC, gave no, or only a modest, suppression of colonic motility evoked by HAS (Figure 3C).

Localization of KCNK9 and KCNK3 proteins

In order to investigate the possible involvement of these KCNK channels in HAS-induced motility, RT-PCR was performed using specific primers for rat KCNK3, KCNK9 and KCNK18. Our results

show that KCNK3 and KCNK9 mRNAs are expressed in the muscle layer, whereas KCNK18 mRNA is barely detectable in the rat proximal colon (Figure 4A). The localization of KCNK3 and KCNK9 was evaluated by ISH and immunohistochemistry. As shown in Figure 4B, KCNK3 mRNA was localized in the longitudinal muscle (LM) layer and myenteric plexus (MP) and KCNK9 mRNA in MP (Figure 4B). A neuronal marker PGP9.5 mRNA co-existed with KCNK9 mRNA (Figure 4B). Immunohistochemistry of whole mount preparation of colonic muscle layers confirmed the predominant localization of KCNK9 in MP and in the enteric nerves in the circular muscle (CM) layer (Figure 5A), and that of KCNK3 in LM SMCs (Figure 5B). Co-immunostaining analysis with anti-KCNK9 and anti-PGP9.5 antibodies (Figure 5C) showed that KCNK9 is expressed in 35.8 % of $PGP9.5^+$ MP cells (n = 148). More than a quarter of $KCNK9^+$ cells in MP are $PGP9.5^-$. Furthermore, in co-immunostaining experiments with KCNK9 and an ICC marker c-kit (Figure 5D), 22.4 % of $c\text{-}kit^+$ cells in MP were found to be $KCNK9^+$ (n = 156) though the double positive cells had relatively weaker c-kit immunosignals (i.e., most of the cells with the strongest c-kit immunosignals lacked KCNK9 immunosignal). Nearly half of $KCNK9^+$ cells in MP were $c\text{-}kit^-$ (often located adjacent to $c\text{-}kit^+$ cells). KCNK9 signals were not detected in PDGFR-α-positive fibroblast-like interstitial cells (data not shown), which are thought to participate in inhibitory neurotransmission of enteric nerves.

HAS induced membrane depolarization via blocking rat KCNK9

283 It is not known whether HAS and HBS inhibit rat KCNK3 and/or KCNK9. Thus, we conducted two
284 electrode voltage clamp assays using *Xenopus* oocytes expressing rat KCNK3 or KCNK9. Because
285 both channels were reported to be regulated by extracellular pH, application of pH6.5 solution was
286 used as a positive control. Inhibitory effect of test compounds were determined with a holding
287 potential of +60 mV. LID was used as a non-selective KCNK channel blocker, which strongly
288 inhibited both KCNK3 and KCNK9. As shown in Figure 6A, HAS showed significant and dose
289 dependent inhibition against KCNK3 and KCNK9 while HBS inhibited only KCNK3. These results
290 were comparable to those observed for murine KCNKs (1).
291 KCNK channels regulate the excitability of cells such as smooth muscle and neurons by adjusting
292 their membrane potential. To address whether HAS inhibition against KCNK3 and KCNK9 led to
293 membrane depolarization, we examined the membrane potential of rat KCNK3- or
294 KCNK9-expressing CHO-K1 cells (Figures 6B, 6C) by using a membrane potential dye. In this
295 assay, the fluorescent signal increases during membrane depolarization and decreases during
296 membrane hyperpolarization. For example, the application of KCl increased the fluorescent signal,
297 which represents a depolarizing membrane potential. The KCl-induced changes in fluorescence
298 intensity for KCNK3 and KCNK9 expressing cells were larger than that observed for the mock cells
299 (Figure 6B). Data are represented by the normalized change in fluorescence ($\Delta F/F_0$). Inhibition of
300 KCNK3 or 9 was determined at 100 seconds after compound application. The application of HAS

and LID to KCNK3- and KCNK9-expressing cells significantly increased the fluorescence intensity. The effect induced by 30 μM of HAS was comparable to that induced by 1 mM of LID, although LID induced depolarization not only in KCNKs-expressing cells but also in mock cells (Figure 6C). HBS appeared to induce depolarization of KCNK3-expressing cells but the effect was not significant (Figures 6B, 6C).

HBS and LID induce colonic motor patterns different from HAS

Although HAS, HBS, and LID raised the intraluminal pressure of rat isolated colons, and induced potent contraction/motility, the resulting motor patterns differed among these three compounds. While the pressure peaks induced by HAS were strong and repeated periodically with almost the same frequency, those induced by HBS were lower in frequency and less periodic (Figure 7A, Supplementary Movie M6). The effects induced by LID were also weaker in amplitude, not periodic, but higher in frequency than those induced by HAS (Figure 7B, Supplementary Movie M7). The spatiotemporal maps also suggested that HAS induces potent motor activity propagating from the oral side to the aboral side over the entire proximal colon (Figure 1A), while LID was found to induce high frequency, low amplitude, non-propulsive motor activity (Figure 7B). Table 1 shows the PF of HAS-, HBS-, and LID-induced colonic motility.

High amplitude contraction by HAS is nerve-mediated.

The contractions induced by 10 μM HAS were suppressed almost completely by addition of TTX

319 (0.3 μM), a neuroleptic agent (Figure 8A). By contrast, the contractions induced by HBS were not
320 abolished but its shape was changed by TTX (Figure 8B). Addition of high doses (up to 3 mM) of
321 TTX did not alter the effect of LID (1 mM, data not shown).

322 **HAS accelerates defecation in normal and POI model rats.**

323 In order to investigate whether HAS accelerates defecation *in vivo* we examined the amount of feces
324 accumulated during a short period after treatment with the agents. The accumulated number of fecal
325 pellets increased significantly at 5 hr after oral administration of 50 mg/kg HAS to normal rats
326 (Figure 9A).

327 For rats that had undergone abdominal surgery, the number of pellets decreased significantly 7 hr
328 after suturing (Figure 9B). Oral administration of HAS at 3 hr after the operation significantly
329 increased the number of pellets 4 hr after administration (i.e., 7 hr after the operation) in a
330 dose-dependent manner (Figure 9C). Accordingly, a single oral administration of TU-100 3 hr after
331 the operation also increased the number of pellets 3 hr after drug treatment (i.e., 6 hr after the
332 operation) in a dose-dependent manner. A significant outcome was obtained at a dose of 3 g/kg
333 TU-100 (Figure 9D).

334

335

DISCUSSION

HAS was found to induce high amplitude of contractions with significant levels of periodicity. The peak frequency (~ 0.5/min), propagating/propulsive property, sensitivity to TTX and the presence of relaxation phase preceding a very strong contractions are in good agreement with those reported for LDC (11). LID, however, was found to induce low amplitude contractions with high frequency (~6/min), which were non-propulsive and insensitive to TTX (i.e., in good agreement with RPR (11)). The increase in amplitude induced by HBS might be periodic, but the interval between consecutive peaks were wider and the incidence of the peaks appeared more irregular compared to those induced by HAS. As shown in Figure 3, “LDC” induced by HAS was not caused by the agonistic activity of TRPV1/TRPA1, which is well documented for HAS and HBS. We reasoned that the target molecules of HAS, HBS and LID may be KCNK channels because these agents, especially HAS and HBS, have a high specificity for KCNK3 and/or KCNK9. Bautista et al (1) have screened various ion channels including KCNK1~6, 9, 10, 13, 16 and 18 and reported specific inhibition of KCNK3 by HBS and of KCNK3/9/18 by HAS. LID blocks a broad range of KCNKs. Although many of the biological activities of LID can be attributed to its inhibitory activity against multiple voltage-gated sodium channels, the effect on KCNK3 has been suggested to be involved in LID-induced seizure in mice (6).

KCNK ion channels comprise a family of potassium-selective channels that share the unique

354 structural feature of four transmembrane domains and two pore-forming domains (8). The KCNK
355 channel family are open across the physiological voltage range and are therefore believed to underlie
356 many of the background K^+ currents (also known as resting, baseline, or leak currents) that regulate
357 the resting membrane potential and excitability of many mammalian cells (2, 7, 21). KCNK channels
358 are found in neuronal and non-neuronal tissues, and they provide, in addition to setting of resting
359 membrane potentials (13, 23), a wide variety of important functions, including sensing of oxygen
360 and pH, neuroprotection, and mechanosensitivity (28). These channels are also candidates for the
361 action of volatile anaesthetics on neural excitability (27). Molecular analysis of GI smooth muscle
362 myocytes revealed expression of KCNK genes, including KCNK2, KCNK10 (14), KCNK3 and
363 KCNK5 (28), and the properties of the currents produced by these channels have been shown to
364 contribute to the native currents observed in GI smooth muscle (4). These data suggest that certain
365 KCNK family channels may be involved in the regulation of GI motility.
366 Interestingly, we found that the KCNK9/KCNK3 blocker HAS evokes a unique motor pattern with a
367 high-degree of periodicity while its geometric isomer, HBS, specifically blocked KCNK3 and
368 induced a motor pattern different from that of HAS. This observation suggests that the highly
369 periodic LDC evoked by HAS may be mediated by KCNK9. In the present study, we show that
370 KCNK3 is located in LM SMC and presumably a small portion of neuronal cells in MP, whereas
371 KCNK9 is located mainly in a portion of neuronal cells in MP and CM layer. These findings are in

good accordance with previous immunohistochemical studies using mouse (14, 28) and human (19) GI tissue. The location of KCNK9 suggests that the channel may be involved in the determination of resting potential and excitability of a substantial portion of enteric neurons innervating the MP and CM layer. The "LDC" induced by HAS was completely abrogated by TTX treatment. If HAS blocks KCNK9 in these motor neurons, their excitability will be augmented. Under such conditions, even if signals with similar intensity are provided from upstream neurons (e.g., interneurons and intrinsic primary afferent neurons) and/or enteroendocrine cells, the strength of the signals to the ICC/SMC will differ substantially. Furthermore, while our data indicates that KCNK9 is not expressed in SMC, it addressed the possibility of its expression in ICC in MP (ICC-MP). ICC-MP network is a pacemaker and has been suggested to actively propagate rhythmic transient depolarizations responsible for RPMC and/or LDC (11, 29). If HAS affects ICC-MP to augment its functions, (i.e., to generate more intense and well-regulated electrical periodicity), the agent would evoke potent and regular "LDC" as demonstrated in the present results.

Because KCNK3 exists predominantly in LM SMC, it is thought to be involved in the regulation of excitability of SMC, which may chiefly affect the tone of muscle contractility. The present study indicates that KCNK3 might be expressed in some neurons in MP. This fiding is intriguing because the effect of HBS, the blocker of KCN3, was not abrogated but its potency and frequency were changed by TTX, suggesting a possible involvement of motility control system of both neurogenic

390 and myogenic origin. Chen et al. (3) has demonstrated that myogenic mechanisms could be involved
391 in certain LDC-like rhythmic activity. Thus, further detailed examination is necessary to clarify the
392 effect of KCNK3 on colonic motility.
393 The properties of the LID-induced motility are in good accordance with those of RPR, which is
394 thought to be mediated by the submuscular ICC (ICC-SMP) network (11). LID is primarily a potent
395 inhibitor of several voltage-gated sodium channels and has a wide array of biological activities
396 including the effects on other KCNK family channels (5, 20) in which the blocking of KCNK3 is
397 only one item of the array. Accordingly, 1 mM LID significantly increased the membrane potential
398 in KCNK3-, KCNK9- and mock-transfected CHO-K1 cells, which strongly suggests that the
399 depolarization by LID may be due to a mechanism other than its inhibition of KCNK3/9.
400 HAS is a major ingredient of TU-100, which has been integrated into the modern medical system
401 under the approval of the Ministry of Health, Labor and Welfare of Japan. Basic research has
402 revealed the various beneficial effects of TU-100 on intestinal motility (9, 30, 32), adhesion (31),
403 vasodilatation (16), and inflammation (15). Clinical trials of TU-100 are currently underway in the
404 U.S. aimed at the development of novel therapeutic treatments for various intestinal disorders. These
405 studies include research on GI and colonic transit by validated scintigraphy, which has indicated
406 TU-100 significantly accelerates ascending colon empting in healthy human volunteers (22).
407 Pharmacokinetics studies have shown that, when TU-100 is administered orally, HAS is rapidly

absorbed in the gut and reaches high concentrations in the blood (approximately 1 μM in human and rats) within 15 min (12, 24, 25). The present experimental settings for the bath application of HAS to the proximal colon is in reasonable agreement with the clinical situation of orally-administered TU-100 in terms of the pharmacological and pharmacokinetic properties of the drug. Furthermore, we have observed that low dosages of HAS, which are too low to induce "LDC" alone, enhance motility triggered by other stimuli such as bethanechol, capsaicin or gingerol (data not shown). This observation is in good accordance with the assumed mechanism of action of HAS, i.e., augmentation of excitability of enteric motor neurons *via* blocking KCNK9.

In order to investigate whether the induction/enhancement of "LDC" *in vitro* relates to the colonic transit *in vivo*, we have examined the effect of HAS or TU-100 on defecation of normal and postoperative rats. A single administration of HAS or TU-100 increased the number of fecal pellets accumulated over a short period of time (3-4 hr after drug treatment and 6-7 hr after surgery).

Although the present study may provide potentially interesting findings, there are several points to be validated and investigated in future studies. Firstly, involvement of KCNK channels in HAS/HBS/LID-mediated motility is still unclear. The use of more specific agonists and/or antagonists, and gene-manipulated mice is necessary to clarify this point. Secondly, further investigation into the biological function of KCNK channels in the generation of slow wave activity, rhythmic transient depolarizations and colonic motility is needed. In the present study, we have

426 demonstrated that KCNK channels strongly affect the membrane potential in the cell line. However,
427 detailed analyses on gastrointestinal cells and tissues, such as the measurement of inhibitory junction
428 potential, have yet to be performed. Thirdly, whether the KCNK9 channel is expressed in ICC-MP
429 should be determined by more conclusive and quantitative methods such as more extensive
430 morphometrical immunohistochemistry of the tissues and analysis of KCNK9 protein and mRNA in
431 purified ICCs. If KCNK9 is expressed in a subpopulation of ICC-MP, it will be reasonable for HAS
432 to modulate the pace-making of colonic motility. Elucidation of these points will undoubtedly
433 contribute to a deeper understanding of the physiology and molecular biology of colonic motor
434 activities.

435 In conclusion, we have demonstrated that HAS may induce or enhance “LDC” of the proximal colon
436 presumably elevating the excitability of enteric nerves *via* KCNK9 blocking. The present findings
437 provide not only a clarification of the mechanism of action of a promising new medicine TU-100,
438 but also a way to develop a novel therapeutic strategy for the treatment of intestinal dysmotility.
439
440
441

REFERENCES

1. **Bautista DM, Sigal YM, Milstein AD, Garrison JL, Zorn JA, Tsuruda PR, Nicoll RA, and Julius D**. Pungent agents from Szechuan peppers excite sensory neurons by inhibiting two-pore potassium channels. *Nat Neurosci* 11: 772-779, 2008.

2. **Bayliss DA, and Barrett PQ**. Emerging roles for two-pore-domain potassium channels and their potential therapeutic impact. *Trends Pharmacol Sci* 29: 566-575, 2008.

3. **Chen JH, Zhang Q, Yu Y, Li K, Liao H, Jiang L, Hong L, Du X, Hu X, Chen S, Yin S, Gao Q, Yin X, Luo H, and Huizinga JD**. Neurogenic and myogenic properties of pan-colonic motor patterns and their spatiotemporal organization in rats. *PloS one* 8: e60474, 2013.

4. **Cho SY, Beckett EA, Baker SA, Han I, Park KJ, Monaghan K, Ward SM, Sanders KM, and Koh SD**. A pH-sensitive potassium conductance (TASK) and its function in the murine gastrointestinal tract. *J Physiol* 565: 243-259, 2005.

5. **Doherty TJ, and Seddighi MR**. Local anesthetics as pain therapy in horses. *Vet Clin North Am Equine Pract* 26: 533-549, 2010.

6. **Du G, Chen X, Todorovic MS, Shu S, Kapur J, and Bayliss DA**. TASK Channel Deletion Reduces Sensitivity to Local Anesthetic-induced Seizures. *Anesthesiology* 115: 1003-1011, 2011.

7. **Enyedi P, and Czirjak G**. Molecular background of leak K+ currents: two-pore domain potassium channels. *Physiol Rev* 90: 559-605, 2010.

8. **Goldstein SA, Bockenhauer D, O'Kelly I, and Zilberberg N**. Potassium leak channels and the KCNK family of two-P-domain subunits. *Nat Rev Neurosci* 2: 175-184, 2001.

9. **Hayakawa T, Kase Y, Saito K, Hashimoto K, Ishige A, Komatsu Y, and Sasaki H**. Effects of Dai-kenchu-to on intestinal obstruction following laparotomy. *J Smooth Muscle Res* 35: 47-54, 1999.

10. **Heredia DJ, Dickson EJ, Bayguinov PO, Hennig GW, and Smith TK**. Localized release of serotonin (5-hydroxytryptamine) by a fecal pellet regulates migrating motor complexes in murine colon. *Gastroenterology* 136: 1328-1338, 2009.

11. **Huizinga JD, Martz S, Gil V, Wang XY, Jimenez M, and Parsons S**. Two independent networks of interstitial cells of cajal work cooperatively with the enteric nervous system to create colonic motor patterns. *Frontiers in neuroscience* 5: 93, 2011.

12. **Iwabu J, Watanabe J, Hirakura K, Ozaki Y, and Hanazaki K**. Profiling of the compounds absorbed in human plasma and urine after oral administration of a traditional Japanese (kampo) medicine, daikenchuto. *Drug Metab Dispos* 38: 2040-2048, 2010.

13. **Kim Y, Bang H, and Kim D**. TASK-3, a new member of the tandem pore K(+) channel family. *J Biol Chem* 275: 9340-9347, 2000.

14. **Koh SD, Monaghan K, Sergeant GP, Ro S, Walker RL, Sanders KM, and Horowitz B**. TREK-1 regulation by nitric oxide and cGMP-dependent protein kinase. An essential role in smooth muscle inhibitory neurotransmission. *J Biol Chem* 276: 44338-44346, 2001.

15. **Kono T, Kaneko A, Hira Y, Suzuki T, Chisato N, Ohtake N, Miura N, and Watanabe T**. Anti-colitis and -adhesion effects of daikenchuto via endogenous adrenomedullin enhancement in Crohn's disease mouse model. *J Crohns Colitis* 4: 161-170, 2010.

16. **Kono T, Kaneko A, Omiya Y, Ohbuchi K, Ohno N, and Yamamoto M**. Epithelial transient receptor potential ankyrin 1 (TRPA1)-dependent adrenomedullin upregulates blood flow in rat small intestine. *Am J Physiol Gastrointest Liver Physiol* 304: G428-436, 2013.

17. **Kono T, Kanematsu T, and Kitajima M**. Exodus of Kampo, traditional Japanese medicine, from the complementary and alternative medicines: is it time yet? *Surgery* 146: 837-840, 2009.

18. **Koo JY, Jang Y, Cho H, Lee CH, Jang KH, Chang YH, Shin J, and Oh U**. Hydroxy-alpha-sanshool activates TRPV1 and TRPA1 in sensory neurons. *Eur J Neurosci* 26: 1139-1147, 2007.

19. **Kovacs I, Pocsai K, Czifra G, Sarkadi L, Szucs G, Nemes Z, and Rusznak Z**. TASK-3 immunoreactivity shows differential distribution in the human gastrointestinal tract. *Virchows Arch* 446: 402-410, 2005.

20. **Lauretti GR**. Mechanisms of analgesia of intravenous lidocaine. *Rev Bras Anestesiol* 58: 280-286, 2008.

21. **Lotshaw DP**. Biophysical, pharmacological, and functional characteristics of cloned and native mammalian two-pore domain K+ channels. *Cell Biochem Biophys* 47: 209-256, 2007.

22. **Manabe N, Camilleri M, Rao A, Wong BS, Burton D, Busciglio I, Zinsmeister AR, and Haruma K**. Effect of daikenchuto (TU-100) on gastrointestinal and colonic transit in humans. *Am J Physiol Gastrointest Liver Physiol* 298: G970-975, 2010.

23. **Millar JA, Barratt L, Southan AP, Page KM, Fyffe RE, Robertson B, and Mathie A**. A functional role for the two-pore domain potassium channel TASK-1 in cerebellar granule neurons. *Proc Natl Acad Sci U S A* 97: 3614-3618, 2000.

24. **Munekage M, Ichikawa K, Kitagawa H, Ishihara K, Uehara H, Watanabe J, Kono T, and Hanazaki K**. Population pharmacokinetic analysis of daikenchuto, a traditional Japanese medicine (Kampo) in Japanese and US health volunteers. *Drug Metab Dispos* 41: 1256-1263, 2013.

513 25. **Munekage M, Kitagawa H, Ichikawa K, Watanabe J, Aoki K, Kono T, and**
514 **Hanazaki K**. Pharmacokinetics of daikenchuto, a traditional Japanese medicine (kampo) after
515 single oral administration to healthy Japanese volunteers. *Drug Metab Dispos* 39: 1784-1788,
516 2011.
517 26. **Nozawa K, Kawabata-Shoda E, Doihara H, Kojima R, Okada H, Mochizuki S,**
518 **Sano Y, Inamura K, Matsushime H, Koizumi T, Yokoyama T, and Ito H**. TRPA1 regulates
519 gastrointestinal motility through serotonin release from enterochromaffin cells. *Proc Natl Acad*
520 *Sci U S A* 106: 3408-3413, 2009.
521 27. **Patel AJ, Honore E, Lesage F, Fink M, Romey G, and Lazdunski M**. Inhalational
522 anesthetics activate two-pore-domain background K+ channels. *Nat Neurosci* 2: 422-426, 1999.
523 28. **Sanders KM, and Koh SD**. Two-pore-domain potassium channels in smooth
524 muscles: new components of myogenic regulation. *J Physiol* 570: 37-43, 2006.
525 29. **Sanders KM, and Ward SM**. Kit mutants and gastrointestinal physiology. *J Physiol*
526 578: 33-42, 2007.
527 30. **Satoh K, Hayakawa T, Kase Y, Ishige A, Sasaki H, Nishikawa S, Kurosawa S,**
528 **Yakabi K, and Nakamura T**. Mechanisms for contractile effect of Dai-kenchu-to in isolated
529 guinea pig ileum. *Dig Dis Sci* 46: 250-256, 2001.
530 31. **Tokita Y, Yamamoto M, Satoh K, Nishiyama M, Iizuka S, Imamura S, and Kase**
531 **Y**. Possible involvement of the transient receptor potential vanilloid type 1 channel in
532 postoperative adhesive obstruction and its prevention by a kampo (traditional Japanese)
533 medicine, daikenchuto. *J Pharmacol Sci* 115: 75-83, 2011.
534 32. **Tokita Y, Yuzurihara M, Sakaguchi M, Satoh K, and Kase Y**. The pharmacological
535 effects of Daikenchuto, a traditional herbal medicine, on delayed gastrointestinal transit in rat
536 postoperative ileus. *J Pharmacol Sci* 104: 303-310, 2007.
537

538 **Figure Legends**

539 **Figure 1.** Induction of colonic motor activity and intraluminal high amplitude pressure by HAS in
540 rat proximal colons. **A.** An entire recording of intraluminal pressure in a representative experiment is
541 shown. A colonic specimen was placed in the bath and video images and intraluminal pressure were
542 taken from time 0 to 4 hr. At 30 min, 10μM of HAS was added, and at 0.75 hr, HAS was washed out
543 by several exchanges with fresh buffer. At 3hr, 10μM of HAS was added again, and at 3.25 hr, HAS
544 was washed out. Moderate amplitude of pressure peaks continued until about 2 hr and thereafter only
545 very small peaks were detected. HAS added at 30 min and 3 hr gave essentially the same motor
546 pattern with similar amplitudes and intervals. **B.** Serial photographs of motility of non-treated (left)
547 and HAS-treated (right) colons. Movie data are shown in Supplementary Movie M3. **C.** Relationship
548 between the intraluminal pressure chart and spatiotemporal map. **Top:** No treatment control (at 3 hr)
549 showing RPMC with low amplitude. **Bottom:** HAS treatment (at 3 hr). A representative example
550 of LDC. Propulsive contractions are displayed as diagonal streaks of dark color. After the addition of
551 HAS, a brief temporal relaxation is frequently observed in the pressure chart (see 10-fold magnified
552 view), but this is always observed by video imaging. The relaxation response is indicated in the
553 figure (labeled “Temporal relaxation”) with the change in minimum pressure levels (labeled by
554 “Basal level down”) before and after HAS application. Non-propulsive contractions are displayed as
555 short, fragmented streaks of dark color. Pink dots in the spatiotemporal map correspond to those in
556 the intraluminal pressure chart.

Figure 2. Dose-dependent induction of high amplitude pressure peaks by HAS. **A.** Typical patterns of intraluminal pressure induced by HAS. WO: wash out. **B.** Quantitation of HAS-induced contractility. %-PF, %-PPA and %-AUC are shown (n = 4 - 6). **P* < .05, ***P* < .01, ****P* < .001 vs. Vehicle control.

Figure 3. Motor activity by HAS is not mediated by TRPV1 nor TRPA1. Typical changes of intraluminal pressure induced by a TRPV1 agonist capsaicin (**A**) and a TRPA1 agonist allyl isothiocyanate (AITC, **B**). **C.** Effects of desensitization (pre-treatment with 3 μM capsaicin plus 10 μM AITC), a TRPV1 antagonist BCTC (1 μM) or a TRPA1 antagonist HC-030031 (5 μM) on HAS-induced motility (n = 5-6). * *P* < .05. "NS", not significant.

Figure 4. Distribution of mRNA of KCNK channels in rat colon. **A.** RT-PCR analysis of mRNA expression in rat colon. PCR products were electrophoresed through a 2 % agarose gel. RT: Reverse transcriptase, SC: Spinal cord. **B.** *In situ* hybridization of rat colon for KCNK3, KCNK9 and PGP9.5. Upper panels represent single staining for KCNK3 or KCNK9. Red dots indicate the target mRNA. Location of the myenteric plexus is indicated by a white-line circle. Lower panels show double staining for PGP9.5 and KCNK9. Red and violet dots indicate PGP9.5 and KCNK9 mRNAs, respectively. KCNK9 mRNA is indicated by arrows. Nuclei were stained with hematoxylin.

Figure 5. Distribution of KCNK9 and KCNK3 proteins in rat colons **A.** Immunohistochemistry of whole-mount muscle layer of rat colon for KCNK9, phalloidin and PGP9.5. LM: Longitudinal

muscle, MP: Myenteric plexus, CM: Circular muscle. **B.** Immunohistochemistry of whole-mount muscle layer of rat colon for KCNK3, phalloidin and PGP9.5. **C**. Double immunostaining of KCNK9 and PGP9.5. in MP. **D**. Double immunostaining of KCNK9 and c-kit in MP. Scale bar = 30 μm.

Figure 6. HAS induces depolarization by blocking KCNK3 and KCNK9. **A.** Two-electrode voltage-clamp analysis with *Xenopus* oocytes expressing rat KCNK3 or KCNK9. Percent suppression of leak current was determined with a holding potential of +60mV. Data are expressed as mean +/- SEM for n=4-8. *p < .05, **p < .01 vs. DMSO control. #p < .05, ###p < .001 vs. PBS control. **B.** Kinetics of the changes of membrane potential responses induced by HAS, HBS and LID using rat KCNK3- or KCNK9-expressing CHO-K1 cells. Application of compounds is indicated by "Apply". Kinetics of the changes in membrane potential responses induced by 90mM KCl is included as a positive control. (n=4) **C.** Summary of normalized response to KCNK3, KCNK9 and mock cell by HAS, HBS and LID. Values represent the ΔF/F0 normalized to that of DMSO or PBS controls (mean +/- SEM for n=4). * p < .05, ** p < .01, ## p < .01.

Figure 7. Motor activity induced by HBS and LID. The typical patterns of HBS (**A**) and LID (**B**) on a spatiotemporal map and intraluminal pressure chart are shown.

Figure 8. The effect of TTX on HAS-, and HBS-induced contraction. **A., B.** Upper charts show typical changes in the HAS (left) and HBS (right) motility patterns induced by TTX. Middle and

593 lower graphs show changes of %-PF, %-PPA and %-AUC induced by TTX, respectively. 10 μM
594 HAS (n = 6) and 30 μM HBS (n = 5 and 6) were used. *P < .05, **P < .01 vs. Control (vehicle).

595 **Figure 9.** The acceleration of defecation by HAS and TU-100 in normal rats or POI model rats. **A.**
596 The increase of defecation frequency at 5 hr after HAS (50 mg/kg p.o.) administration in normal rats.
597 *P < .05, **P < .01 vs Vehicle (olive oil 0.5 mL/kg p.o.) (n=8). **B.** The decrease of defecation
598 frequency by laparotomy. *P < .05, ***P < .001 vs Normal (anesthetized only). (n = 8 ~21, at 7 hrs
599 after operation). **C.** The increase of defecation frequency after HAS (15 and 50 mg/kg p.o.) dosing at
600 4 hrs after administration (i.e., 6 hrs after operation) in POI rats. * P < .05 vs Vehicle (n = 23-25). **D.**
601 The acceleration of defecation frequency induced TU-100 (1 and 3 g/kg p.o.) dosing 3 hrs after
602 administration (i.e., 6 hrs after operation) in POI rats. *, ** P < .05, .01 vs Vehicle (water 15 mL/kg
603 p.o.) (n = 8 or 9).
604

Table 1. Peak frequency of HAS, HBS and LID

Agents	None	None	HAS (10μM)	HBS (30μM)	LID(1mM)
Measured time	0 - 0.25 hr	3 - 3.25 hr	3 - 3.25 hr	3 - 3.25 hr	3 - 3.25 hr
Peak Frequency (number/min)	3.00 ± 0.41	1.27 ± 0.20	0.44 ± 0.03	0.21 ± 0.03	5.64 ± 0.66

The number of peaks during a set period of time was counted in the pressure peak chart and peak frequency (PF) was calculated as the number of peaks per minute. N = 4 – 7.

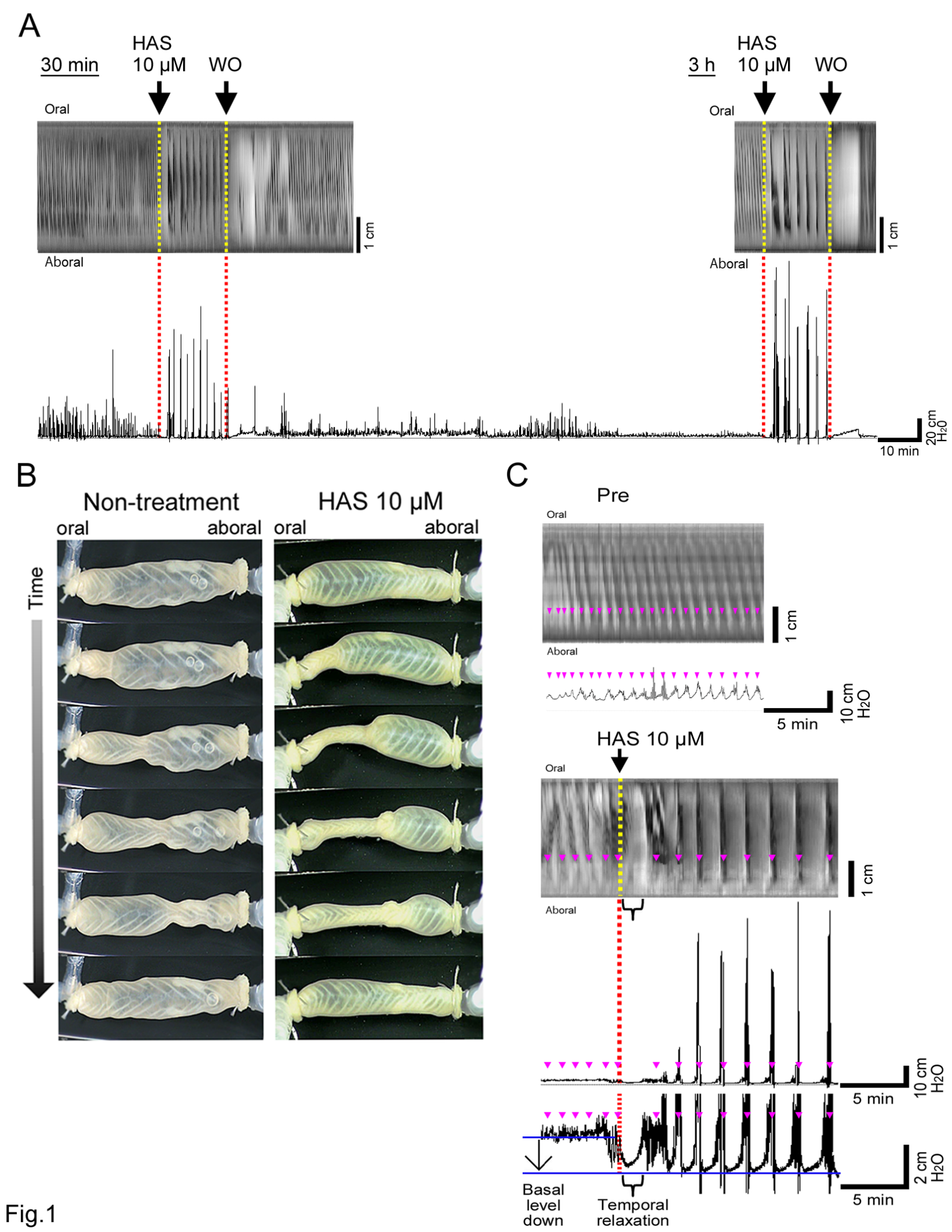
A
30 min
HAS
10 μM
WO
Oral
1 cm
Aboral
3 h
HAS
10 μM
WO
Oral
1 cm
Aboral
20 cm H2O
10 min
B
Non-treatment
oral
aboral
HAS 10 μM
oral
aboral
Time
C
Pre
Oral
1 cm
Aboral
10 cm H2O
5 min
HAS 10 μM
Oral
1 cm
Aboral
10 cm H2O
5 min
2 cm H2O
5 min
Basal level down
Temporal relaxation

Fig.1

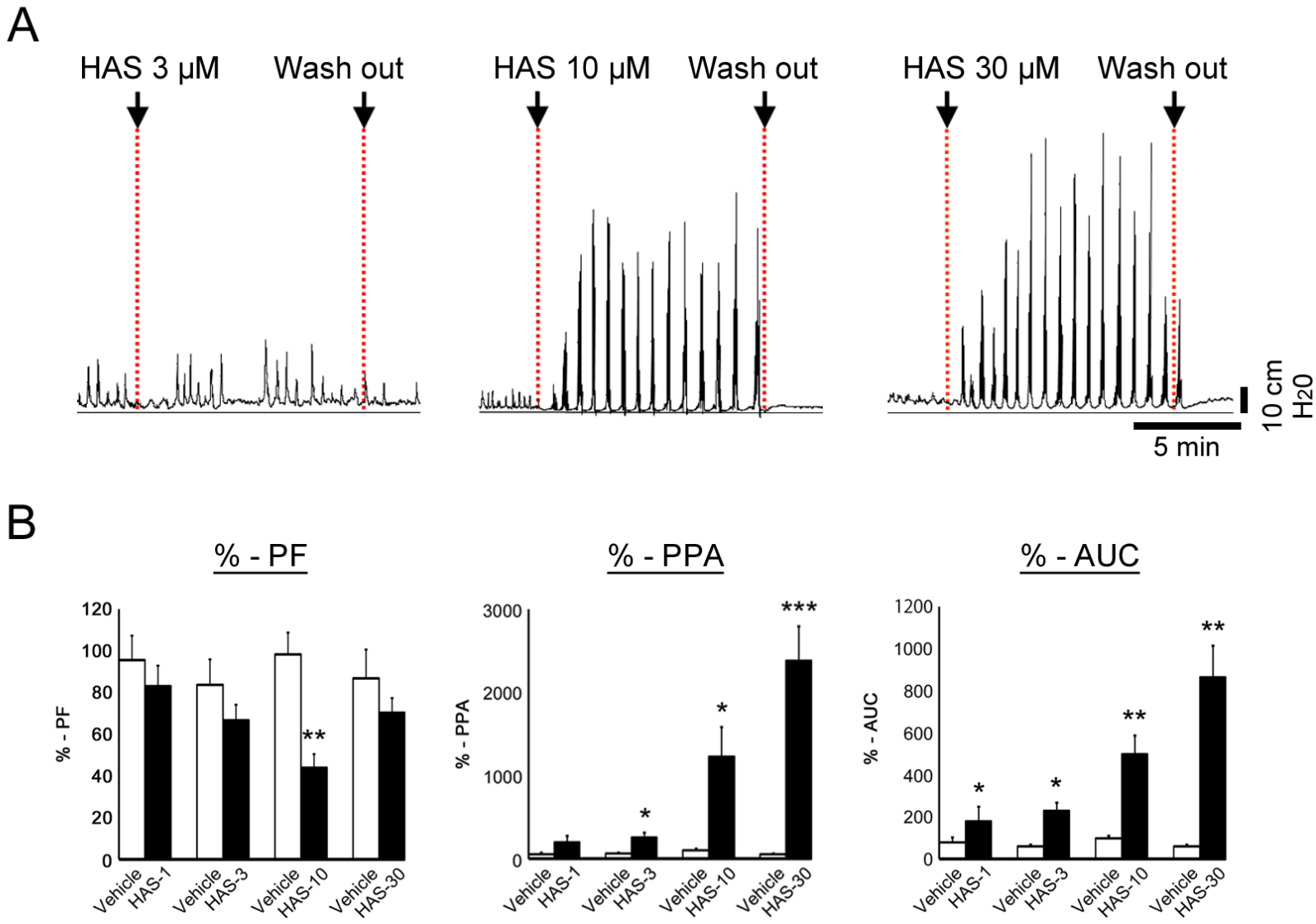
A
HAS 3 µM
Wash out
HAS 10 µM
Wash out
HAS 30 µM
Wash out
10 cm
H20
5 min
B
% - PF
% - PPA
% - AUC
% - PF
% - PPA
% - AUC
Vehicle
HAS-1
HAS-3
HAS-10
HAS-30

Fig.2

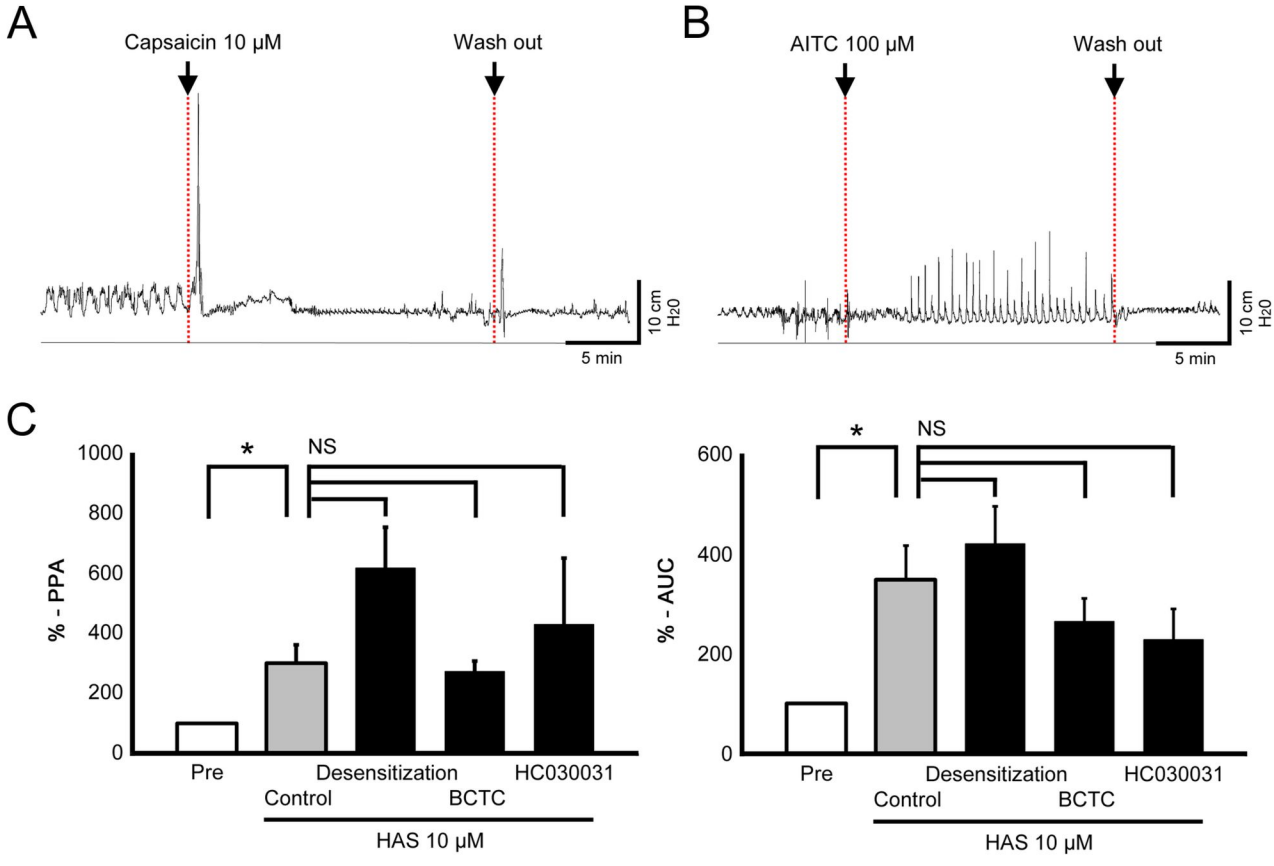
A
Capsaicin 10 μM
Wash out
10 cm H20
5 min
B
AITC 100 μM
Wash out
10 cm H20
5 min
C
% - PPA
1000
800
600
400
200
0
*
NS
Pre
Desensitization
Control
BCTC
HC030031
HAS 10 μM
% - AUC
600
400
200
0
*
NS
Pre
Desensitization
Control
BCTC
HC030031
HAS 10 μM

Fig3

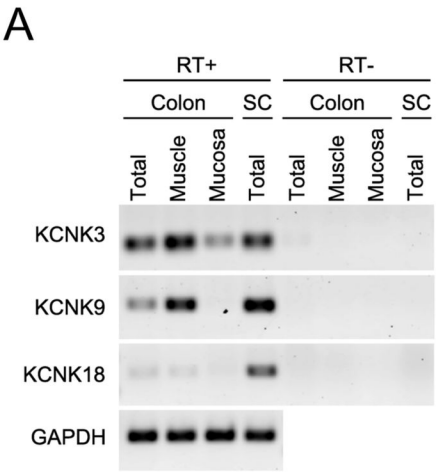
A
RT+
RT-
Colon
SC
Colon
SC
Total
Muscle
Mucosa
Total
Total
Muscle
Mucosa
Total
KCNK3
KCNK9
KCNK18
GAPDH

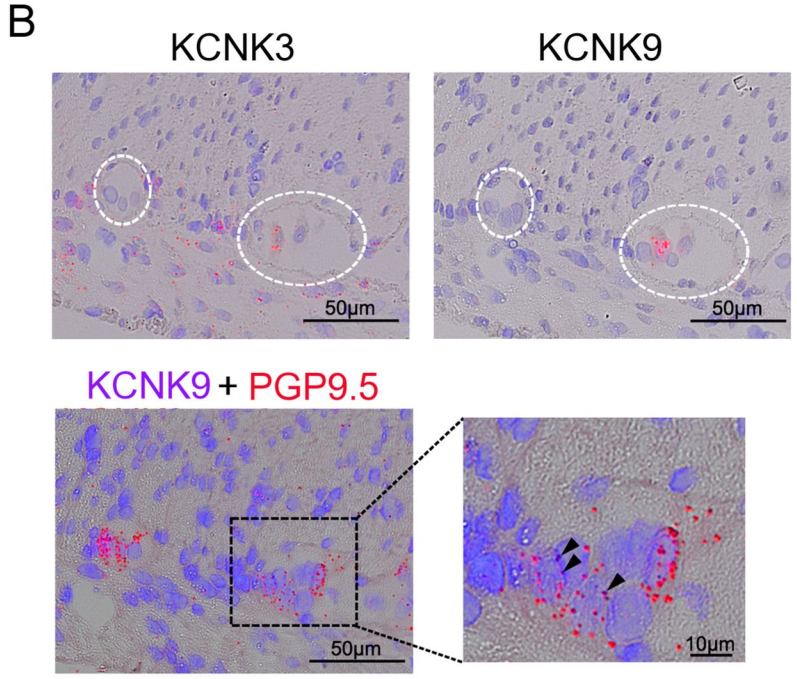
B
KCNK3
KCNK9
50μm
50μm
KCNK9 + PGP9.5
50μm
10μm

Fig4

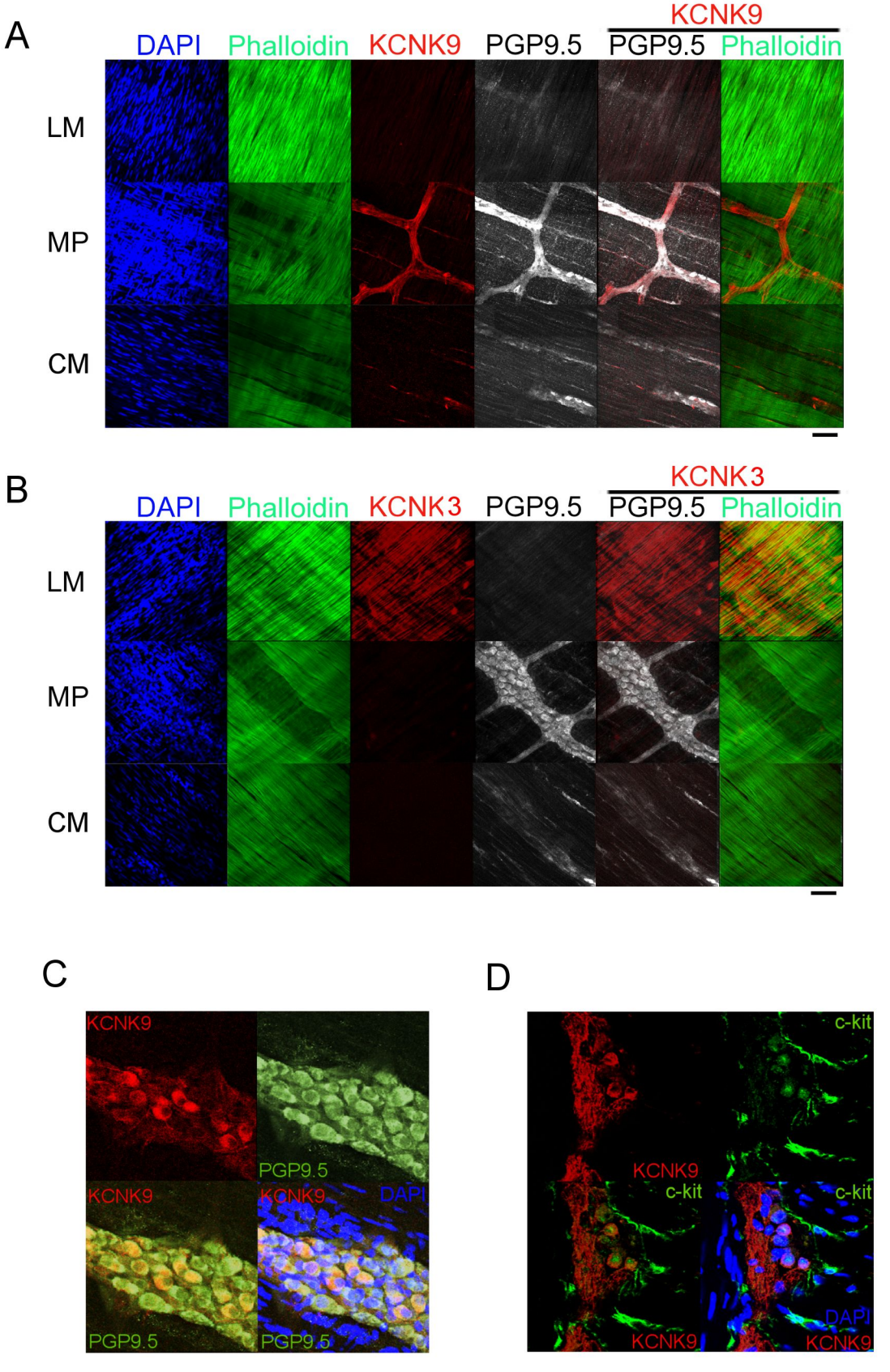
A
DAPI
Phalloidin
KCNK9
PGP9.5
KCNK9
PGP9.5
Phalloidin
LM
MP
CM
B
DAPI
Phalloidin
KCNK3
PGP9.5
KCNK3
PGP9.5
Phalloidin
LM
MP
CM
C
KCNK9
PGP9.5
KCNK9
KCNK9
DAPI
PGP9.5
PGP9.5
D
c-kit
KCNK9
c-kit
c-kit
DAPI
KCNK9
KCNK9

Fig.5

A

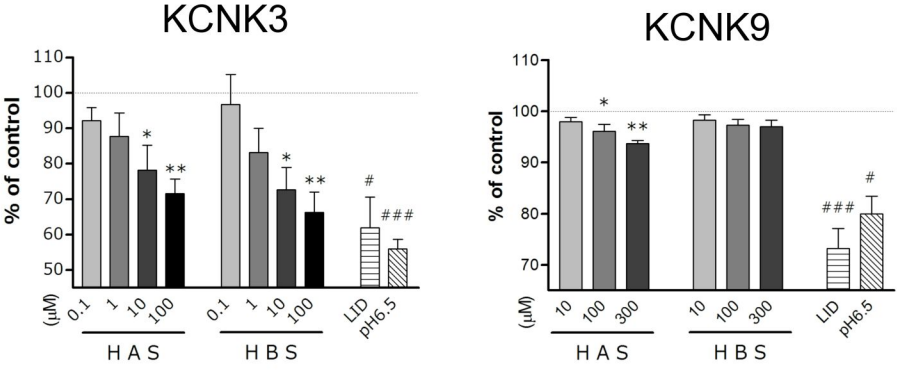

B

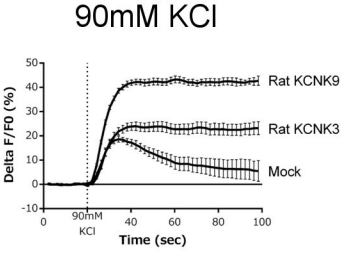

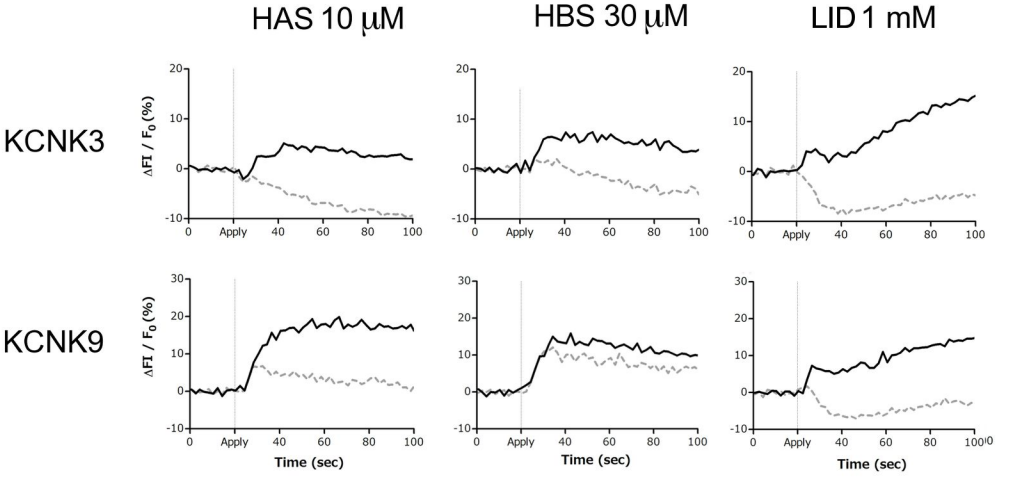

C

Compound	Concentration	KCNK3	KCNK9	Mock
HAS	1.25 μM	−0.7 ± 1.3	−1.8 ± 2.3	−0.2 ± 1.5
	6 μM	1.6 ± 2.0	1.6 ± 1.5	2.8 ± 1.8
	30 μM	11.2 ± 3.8 *	13.6 ± 1.1 **	8.0 ± 2.2
HBS	1.25 μM	3.95 ± 2.7	−1.5 ± 2.3	0.54 ± 1.5
	6 μM	−0.7 ± 2.6	−6.8 ± 3	−1.1 ± 1.4
	30 μM	9.72 ± 3.8	4.25 ± 3	3.09 ± 1.3
Lidocaine	0.2 mM	6.7 ± 0.9	4.04 ± 0.5	11.5 ± 0.5
	1 mM	20.2 ± 0.8 ##	17.1 ± 1.2 ##	22.8 ± 2.0 ##
	5 mM	55.9 ± 4.3 ##	68.9 ± 5.7 ##	46.3 ± 5.9 ##

Fig.6

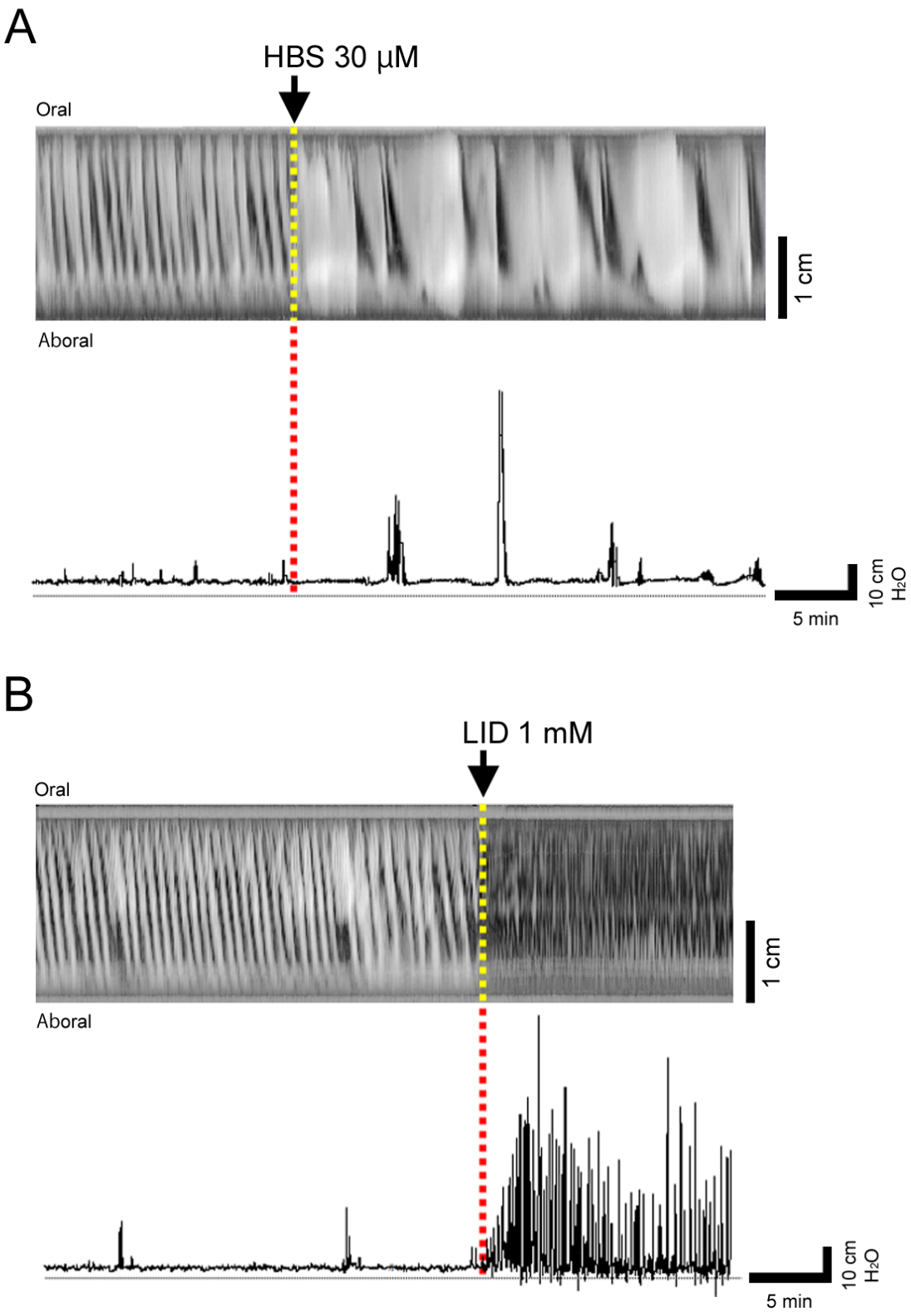
A
HBS 30 µM
Oral
Aboral
1 cm
10 cm
H2O
5 min
B
LID 1 mM
Oral
Aboral
1 cm
10 cm
H2O
5 min

Fig.7

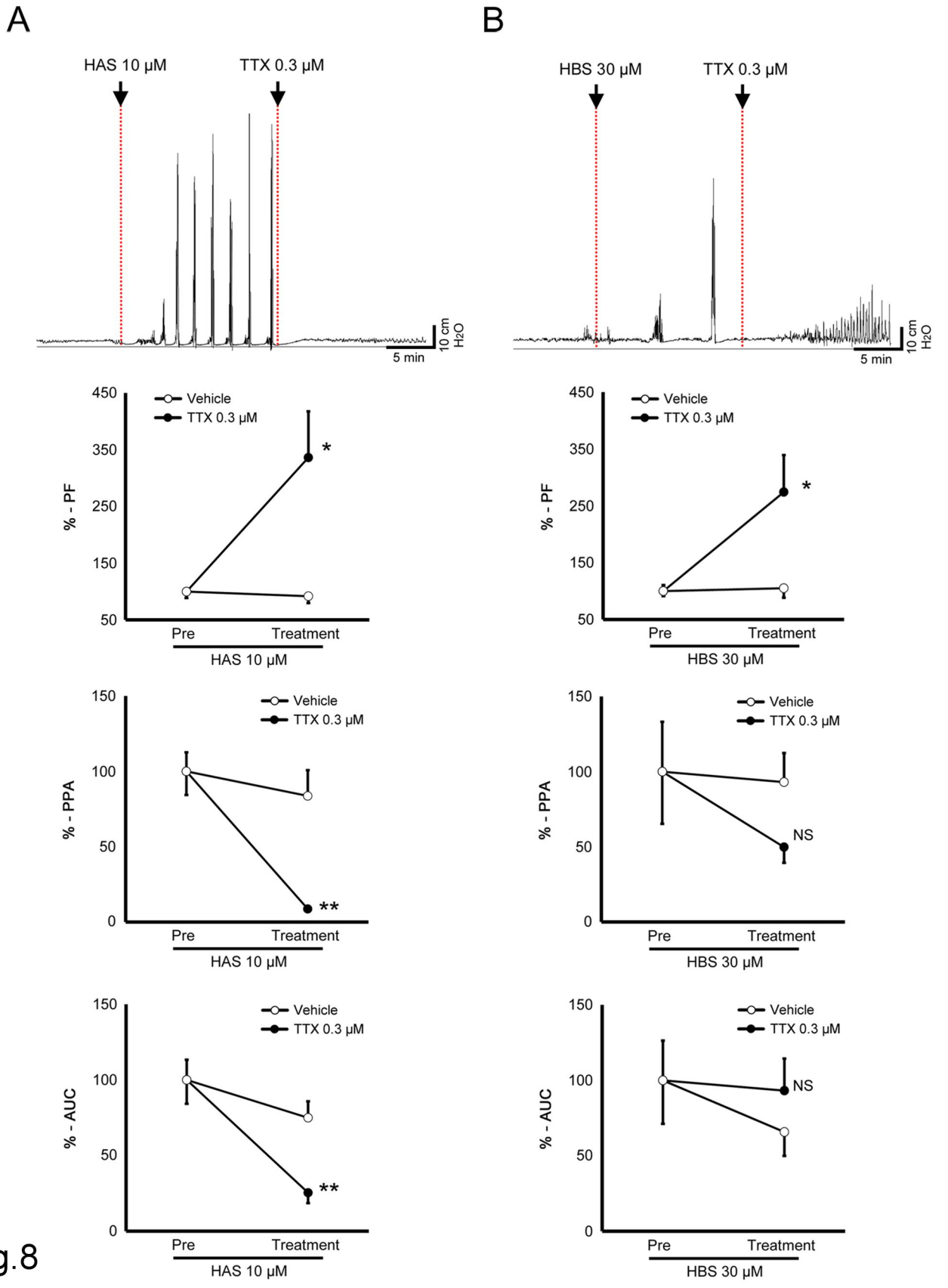
A
HAS 10 μM
TTX 0.3 μM
10 cm
H2O
5 min
B
HBS 30 μM
TTX 0.3 μM
10 cm
H2O
5 min
Vehicle
TTX 0.3 μM
% - PF
450
350
250
150
50
*
Pre
Treatment
HAS 10 μM
HBS 30 μM
% - PPA
150
100
50
0
**
NS
% - AUC

Fig.8

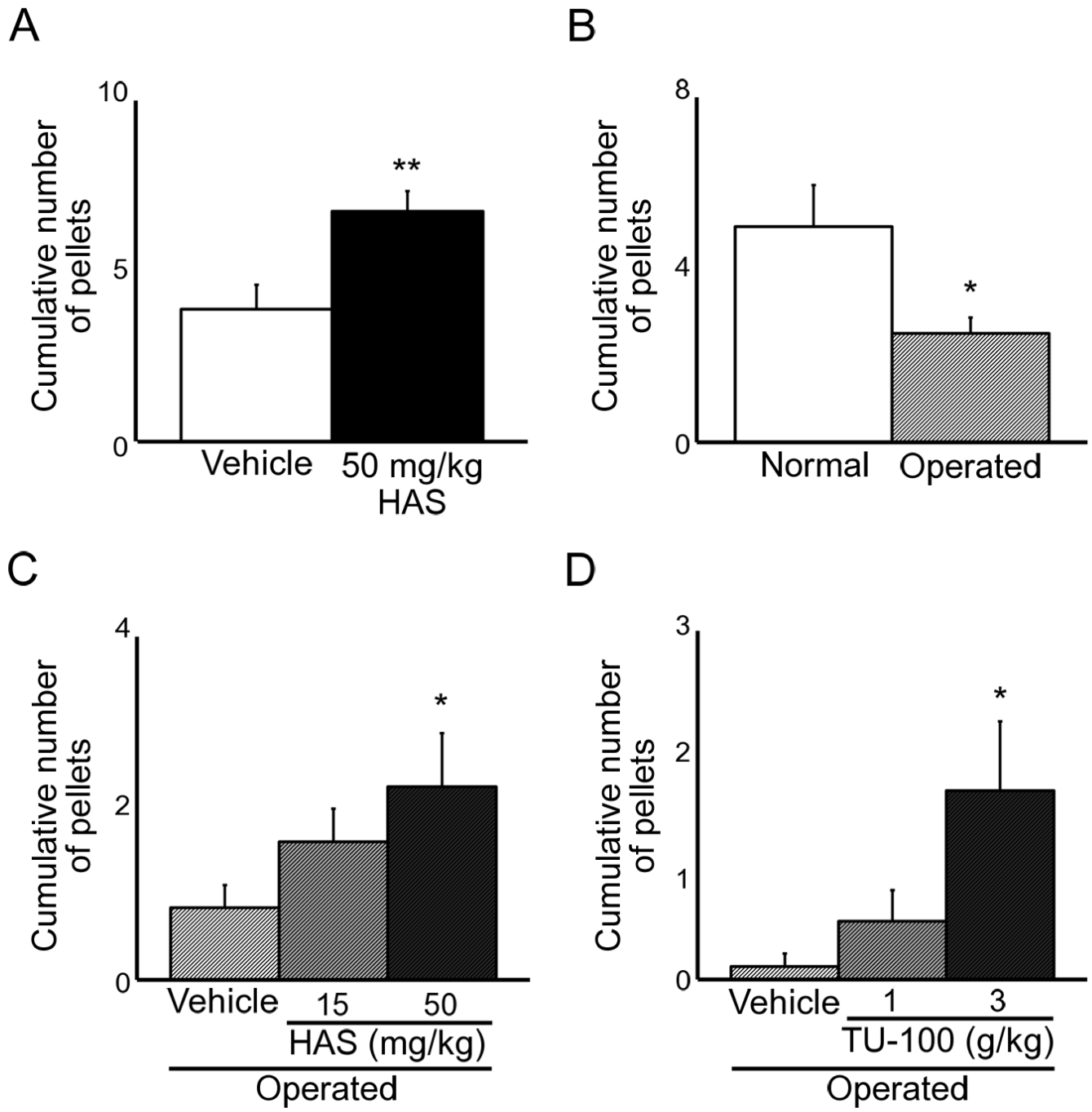
A
Cumulative number of pellets
10
5
0
**
Vehicle
50 mg/kg HAS
B
Cumulative number of pellets
8
4
0
*
Normal
Operated
C
Cumulative number of pellets
4
2
0
*
Vehicle
15
50
HAS (mg/kg)
Operated
D
Cumulative number of pellets
3
2
1
0
*
Vehicle
1
3
TU-100 (g/kg)
Operated

Fig. 9